Single Crystal Structure of Pure Inorganic Nanocomposite $[GaO_4Al_{12}(OH)_{24}(H_2O)_{12}][Al(OH)_6Mo_6O_{18}]_2(OH)\cdot 30H_2O$

Jung-Ho Son and Young-Uk Kwon*

Department of Chemistry and BK-21 School of Science, Sungkyunkwan University (SKKU), Suwon 440-746, Korea
Received July 4, 2001

Single crystals of nanocomposite $[GaO_4Al_{12}(OH)_{24}(H_2O)_{12}][Al(OH)_6Mo_6O_{18}]_2(OH)\cdot 30H_2O$, **2**, were obtained by the reaction between $[GaO_4Al_{12}(OH)_{24}(H_2O)_{12}]^{7+}$ and $[Mo_7O_{24}]^{6-}$ clusters in an aqueous solution, analogously to the $[AlO_4Al_{12}(OH)_{24}(H_2O)_{12}][Al(OH)_6Mo_6O_{18}]_2(OH)\cdot 29.5H_2O$ nanocomposite, **1**. The crystal structure of **2** was determined by single crystal x-ray diffraction; space group *C*2/*c* (No. 15), a = 27.418(2) Å, b = 15.647(2) Å, c = 23.960(4) Å, β = 102.850(9)°, V = 10,021.5(20) Å^3, Z = 4. Detailed analysis of the structural data show that the clusters are held by intimate hydrogen bondings of the surface O^{2-} and OH^- groups of the clusters as well as the ionic interactions between the oppositely charged cluster ions.

Keywords : Polyoxometalate, Nanocomposite, Cluster, Crystal structure.

Introduction

Materials with nanometer sized features are attracting ever increasing attention. Many different approaches like sol-gel, template and intercalation have been adapted for this purpose.[1] Many of these studies demonstrate promising results with unusual physical properties that can be utilized in many fields, for example, electronics, biology, ceramics, optics, etc.[2] However, most of the nanocomposite materials reported so far are limited to organic-organic or organic-inorganic combinations.[3] Nanocomposite containing organic parts may have problems of low thermal stability; purely inorganic nanocomposite materials can be of great help for this problem.

Recently, we have demonstrated that pure inorganic-inorganic nanocomposites can be obtained by combining oppositely charged polyoxometalate clusters. By reacting a Keggin-type polycation $[AlO_4Al_{12}(OH)_{24}(H_2O)_{12}]^{7-}$ (hereafter Al_{13}) and $[V_{10}O_{28}]^{6-}$ (V_{10}) clusters in an aqueous solution, we were able to synthesize monolithic gels in which the individual cluster identities were more or less preserved.[4] By reacting Al_{13} with $[Mo_7O_{24}]^{6-}$ (Mo_7) cluster, we also have obtained single crystals of $[AlO_4Al_{12}(OH)_{24}(H_2O)_{12}][Al(OH)_6Mo_6O_{18}]_2(OH)\cdot 29.5H_2O$ ($Al_{13}(AlMo_6)_2$), **1**, in which the cluster ions are regularly packed only by ionic interactions as in the ionic crystals.[5] The Anderson-type $[Al(OH)_6Mo_6O_{18}]^{3-}$ ($AlMo_6$) heteropolyoxometalate cluster in this compound was generated from the reaction between Al_{13} and Mo_7 clusters.[6] The crystal structure of **1** shows that the Al_{13} and $AlMo_6$ clusters are disposed in such a way to maximize the ionic interactions between the clusters. It also shows an interconnected channel structure that may find applications in the fields of catalysts and sorption materials. With slightly different synthesis conditions, the Al_{13}-Mo_7 system produced powders or monolithic gels as in the Al_{13}-V_{10} system.[7] The Al_{13} clusters in the gels convert into polymerized forms similar to $[Al_{30}O_8(OH)_{56}(H_2O)_{24}]^{18+}$ (Al_{30}) or AlP_2 clusters when Mo/Al ratio is small, as found by the solid state ^{27}Al NMR technique. The polymerization or condensation behavior of Al_{13} is well documented in the literatures.[8] On the other hand, $[GaO_4Al_{12}(OH)_{24}(H_2O)_{12}]^{7-}$ ($GaAl_{12}$) cluster with Ga in place of the central tetrahedral Al site of the Al_{13} is reported not to undergo such condensation reaction into Al_{30} or AlP_2, giving rise to the possibility of monolithic gels with the cluster identities completely unchanged.[9] In addition, $GaAl_{12}$-$AlMo_6$ composite material is expected to show higher thermal stability than Al_{13}-$AlMo_6$ composite because of the reported higher thermal stability of $GaAl_{12}$ over Al_{13}.[9] Thus we have initiated the reaction between the $GaAl_{12}$ and Mo_7 clusters and obtained single crystals of $[GaO_4Al_{12}(OH)_{24}(H_2O)_{12}][Al(OH)_6Mo_6O_{18}]_2(OH)\cdot 30H_2O$, **2**, an $Al_{13}(AlMo_6)_2$ analogue. In this paper, we describe the crystal structure of this compound and compare it with that of **1**. The details of the cluster ion packing structure of **1** and **2** show that the packing is governed by many factors in addition to the ionic interaction between cluster ions. The crystal structures of **1** and **2** will provide insight into the microstructures of the monolithic gels in these and other cluster-cluster nanocomposite systems.

Experimental Section

Synthesis. The $GaAl_{12}$ clusters were synthesized analogously to the Al_{13} clusters as in the literature.[10] A 2.5 M NaOH solution was added dropwisely into an aqueous solution containing 0.24 M $AlCl_3\cdot 6H_2O$ and 0.02 M $Ga(NO_3)_3$ with vigorous stirring until OH/(Al+Ga) ratio reached 2.4-2.5. The solution became increasingly turbid with the NaOH addition. This solution was aged in an oven at 85 °C for 4.5h and finally became clear. A 0.02 M Mo_7 solution was prepared by dissolving $(NH_4)_6Mo_7O_{24}\cdot 4H_2O$ in water with warming. The Mo_7 solution was poured into the $GaAl_{12}$ solution with stirring to make the approximate composition of Al/Mo = 1.17 and immediate precipitate formation was observed. Upon standing undisturbed over a few days, there formed needle-like colorless crystals in the solution. These

crystals were isolated from the remaining precipitate by decantation and washed with water. ICP elemental analysis was performed by Jobin-Yvon 138 Ultrace model. Anal. calcd. ratio : Ga, 1; Al, 14; Mo, 12. Found : Ga, 1; Al, 13.23; Mo, 11.42.

Single crystal X-ray diffraction. A colorless transparent crystal ($0.44 \times 0.36 \times 0.32$ mm^3) was attached on a glass fiber and mounted on a Bruker P4 diffractometer equipped with graphite monochromated Mo-Kα radiation ($\lambda = 0.71073$ Å). A set of 25 reflections randomly found and located were fitted to a monoclinic unit cell with a = 27.418(2) Å, b = 15.647(2) Å, c = 23.960(4) Å, β = 102.850(9)°, V = 10,021.5 (20) Å^3. The systematic absence condition of hkl: h+k = 2n+1 and h0l: l = 2n+1 suggested space groups $C2/c$ and Cc. The intensity statistics and the final structure refinement show that the centrosymmetric $C2/c$ space group is the correct one. The intensity data were corrected for absorption with psi-scan data. The positional parameters of the metal atoms and most of the cluster oxygen atoms were determined by the direct method (SHELXS-86).[11] Several cycles of refinements and difference Fourier syntheses (SHELXL-97-2)[12] revealed the other oxygen atoms of the clusters and lattice water. The final least-squares full matrix refinement on 8760 reflections with 709 variables with no restraints gave $R_1 = 0.0390$ and $wR_2 = 0.1088$ ($I > 2\sigma$) and $R_1 = 0.0420$ and $wR_2 = 0.1114$ (all data). All the atoms were refined anisotropically. The hydrogen atoms were not included in the refinement. Crystallographic data and atomic coordinates of crystal **2** are summarized in Tables 1 and 2, respectively.

Table 1. Crystal data and structure refinement for $[GaO_4Al_{12}(OH)_{24}(H_2O)_{12}][Al(OH)_6Mo_6O_{18}]_2(OH)\cdot 30H_2O$

Identification code	$[GaO_4Al_{12}(OH)_{24}(H_2O)_{12}]$ $[Al(OH)_6Mo_6O_{18}]_2(OH)\cdot 30H_2O$
Empirical formula	Al14 Ga1 Mo12 O118.15
Formula weight	3489.20
Temperature	296(2) K
Wavelength	0.71073 Å
Crystal system	Monoclinic
Space group	$C2/c$
Unit cell dimensions	a = 27.418(2) Å α = 90°
	b = 15.647(2) Å β = 102.850(9)°
	c = 23.960(4) Å γ = 90°
Volume	10022(2) Å^3
Z	4
Density (calculated)	2.313 g·cm^{-3}
Absorption coefficient	1.982 mm^{-1}
Absorption correction method	psi scan
F(000)	6649
Crystal size	$0.44 \times 0.36 \times 0.32$ mm^3
Theta range for data collection	1.82 to 25.00°
Index ranges	-32 <= h <= 0, -18 <= k <= 0, -27 <= l <= 28
Reflections collected	8960
Independent reflections	8760 [R(int) = 0.0143]
Refinement method	Full-matrix least-squares on F^2
Data / restraints / parameters	8760 / 0 / 709
Goodness-of-fit on F^2	1.071
Final R indices [I>2sigma(I)]	$R_1 = 0.0390$, $wR_2 = 0.1088$
R indices (all data)	$R_1 = 0.0420$, $wR_2 = 0.1114$
	$w = 1/[\sigma^2(F_o^2)+(0.0597*P)^2+72.62*P]$
	where $P=(Max(F_o^2,0)+2*F_c^2)/3$
Largest diff. peak and hole	1.388 e·Å^{-3} at 0.1019 0.1316 0.2104 [1.27 Å from OW4]
	-0.897 e·Å^{-3} at 0.1989 0.9458 0.4379 [0.72 Å from Mo5]

Results and Discussion

As in the synthesis of compound **1**, single crystals of compound **2** were obtained through the generation of $AlMo_6$ clusters from the reaction between Mo_7 and $GaAl_{12}$ clusters. In case of compound **1**, the formation of $AlMo_6$ clusters was well accounted for with the reported reactions between Mo_7 clusters with Al_2O_3 and $Al(OH)_3$ because the Al_{13} clusters are intermediate species in the hydrolysis and condensation reaction of Al^{3+} ions in aqueous media.[6] $GaAl_{12}$ clusters are reportedly more stable than Al_{13}. However, this stability is established only with respect to dimerization of the clusters into AlP_2 or Al_{30} clusters.[9] The stability of $GaAl_{12}$ for the decomposition reaction in the presence of Mo_7 into $AlMo_6$ clusters is not well studied. Apparently the same obser-

Table 2. Atomic coordinates ($\times 10^4$) and equivalent isotropic displacement parameters (Å$^2 \times 10^3$) for $[GaO_4Al_{12}(OH)_{24}(H_2O)_{12}]$-$[Al(OH)_6Mo_6O_{18}]_2(OH)\cdot 30H_2O$. U(eq) is defined as one third of the trace of the orthogonalized Uij tensor

	x	y	z	U(eq)	sof
Al(1)	0	5000	5000	21(1)	0.50000
Mo(1)	454(1)	6377(1)	4237(1)	29(1)	1.00000
Mo(2)	1127(1)	4839(1)	4823(1)	29(1)	1.00000
Mo(3)	705(1)	3402(1)	5611(1)	30(1)	1.00000
O(1)	580(1)	5675(2)	5028(1)	26(1)	1.00000
O(2)	387(1)	4103(2)	4773(1)	26(1)	1.00000
O(3)	-217(1)	5477(2)	4247(1)	26(1)	1.00000
O(4)	955(1)	7049(3)	4423(2)	41(1)	1.00000
O(5)	197(2)	6578(3)	3521(2)	39(1)	1.00000
O(6)	794(1)	5343(2)	4086(1)	31(1)	1.00000
O(7)	-28(1)	7027(2)	4556(2)	31(1)	1.00000
O(8)	1345(1)	3988(3)	4491(2)	39(1)	1.00000
O(9)	1626(1)	5510(3)	5021(2)	42(1)	1.00000
O(10)	1162(1)	4315(2)	5564(2)	32(1)	1.00000
O(11)	883(2)	3199(3)	6325(2)	43(1)	1.00000
O(12)	957(2)	2604(2)	5277(2)	41(1)	1.00000
Al(2)	2500	2500	0	24(1)	0.50000
Mo(4)	-3227(1)	3675(1)	5622(1)	34(1)	1.00000
Mo(5)	-3159(1)	4080(1)	4289(1)	38(1)	1.00000
Mo(6)	-2452(1)	2875(1)	3656(1)	34(1)	1.00000
O(21)	-3174(1)	2874(2)	4841(1)	27(1)	1.00000
O(22)	-2437(1)	3130(2)	5691(1)	28(1)	1.00000
O(23)	-2395(1)	3455(2)	4554(1)	28(1)	1.00000
O(24)	-3865(2)	3755(3)	5427(2)	50(1)	1.00000

Table 2. Continued

	x	y	z	U(eq)	sof
O(25)	-3047(2)	4316(3)	6206(2)	53(1)	1.00000
O(26)	-3205(1)	2565(2)	5978(2)	35(1)	1.00000
O(27)	-3026(2)	4428(2)	5078(2)	40(1)	1.00000
O(28)	-2938(2)	4971(3)	4013(2)	61(1)	1.00000
O(29)	-3793(2)	4176(3)	4118(2)	60(1)	1.00000
O(30)	-3109(1)	3238(3)	3708(2)	40(1)	1.00000
O(31)	-2236(2)	3766(3)	3374(2)	48(1)	1.00000
O(32)	-2617(2)	2175(3)	3102(2)	56(1)	1.00000
Ga(1)	0	2578(1)	2500	21(1)	0.50000
Al(11)	477(1)	4566(1)	2357(1)	22(1)	1.00000
Al(12)	712(1)	3254(1)	1588(1)	22(1)	1.00000
Al(13)	1208(1)	3247(1)	2806(1)	26(1)	1.00000
Al(14)	978(1)	1926(1)	3546(1)	29(1)	1.00000
Al(15)	-7(1)	1931(1)	1155(1)	25(1)	1.00000
Al(16)	243(1)	591(1)	3098(1)	31(1)	1.00000
O(41)	508(1)	3289(2)	2338(1)	21(1)	1.00000
O(42)	262(1)	1881(2)	3134(1)	25(1)	1.00000
O(51)	534(1)	5804(2)	2332(2)	33(1)	1.00000
O(52)	960(1)	3382(2)	914(2)	31(1)	1.00000
O(53)	1904(1)	3371(3)	3160(2)	45(1)	1.00000
O(54)	1634(2)	1825(3)	4045(2)	50(1)	1.00000
O(55)	171(1)	1859(2)	414(2)	32(1)	1.00000
O(56)	289(2)	-629(3)	3230(2)	54(1)	1.00000
O(61)	1123(1)	4437(2)	2785(1)	27(1)	1.00000
O(62)	670(1)	4458(2)	1651(1)	24(1)	1.00000
O(63)	197(1)	4581(2)	2997(1)	24(1)	1.00000
O(64)	652(1)	2082(2)	1514(1)	27(1)	1.00000
O(65)	1336(1)	3197(2)	2077(1)	27(1)	1.00000
O(66)	34(1)	3162(2)	1175(1)	24(1)	1.00000
O(67)	994(1)	3115(2)	3489(1)	30(1)	1.00000
O(68)	1225(1)	2068(2)	2894(2)	33(1)	1.00000
O(69)	-683(1)	1944(2)	820(1)	31(1)	1.00000
O(70)	906(1)	746(2)	3460(2)	35(1)	1.00000
O(71)	6(1)	751(2)	1242(2)	35(1)	1.00000
O(72)	385(2)	529(2)	2372(2)	38(1)	1.00000
OW1	1617(2)	5182(3)	1632(2)	59(2)	0.99805
OW2	1713(2)	5809(4)	3728(2)	71(2)	1.00000
OW3	1500(2)	6253(5)	2511(3)	86(3)	0.92575
OW4	1326(3)	734(5)	2041(3)	116(3)	1.00000
OW5	903(3)	7766(7)	3084(3)	127(5)	0.97348
OW6	458(4)	8239(5)	1944(4)	126(5)	0.95731
OW7	2372(4)	4222(7)	4347(7)	178(8)	0.92696
OW8	2400(5)	4728(9)	2931(4)	176(8)	0.85547
OW9	642(8)	272(11)	4885(6)	347(15)	1.00000
OW10	780(7)	9532(10)	1101(9)	198(11)	0.82123
OW11	2169(6)	518(12)	2840(8)	128(9)	0.54895
OW12	2447(6)	7083(11)	1755(11)	236(16)	0.90413
OW13	1703(10)	8746(15)	113(8)	142(12)	0.47891
OW14	1642(9)	8012(15)	1982(12)	291(21)	0.76752
OW15	2003(10)	7584(35)	21(16)	357(46)	0.56401
OW16	2405(15)	6549(28)	1012(27)	180(41)	0.35952
OW17	1778(17)	9450(23)	2616(11)	444(38)	0.75808
OW18	2139(10)	6816(41)	472(20)	239(42)	0.46333
OW19	1569(27)	8673(33)	1074(18)	694(84)	0.77973

vations on the formation processes of crystals **1** and **2** indicate that the reactivity of $GaAl_{12}$ with Mo_7 clusters to form $AlMo_6$ clusters is not significantly different from that of Al_{13}. On the other hand, the crystals of compound **2** tend to be two to three times larger than those of compound **1**. Because the two crystals are isostructural to each other, these observations imply that the formation of $AlMo_6$ from $GaAl_{12}$ is slower than from Al_{13}, which may be related with their respective stabilities.

The crystal **2** is isostructural to **1**, and its crystal structure

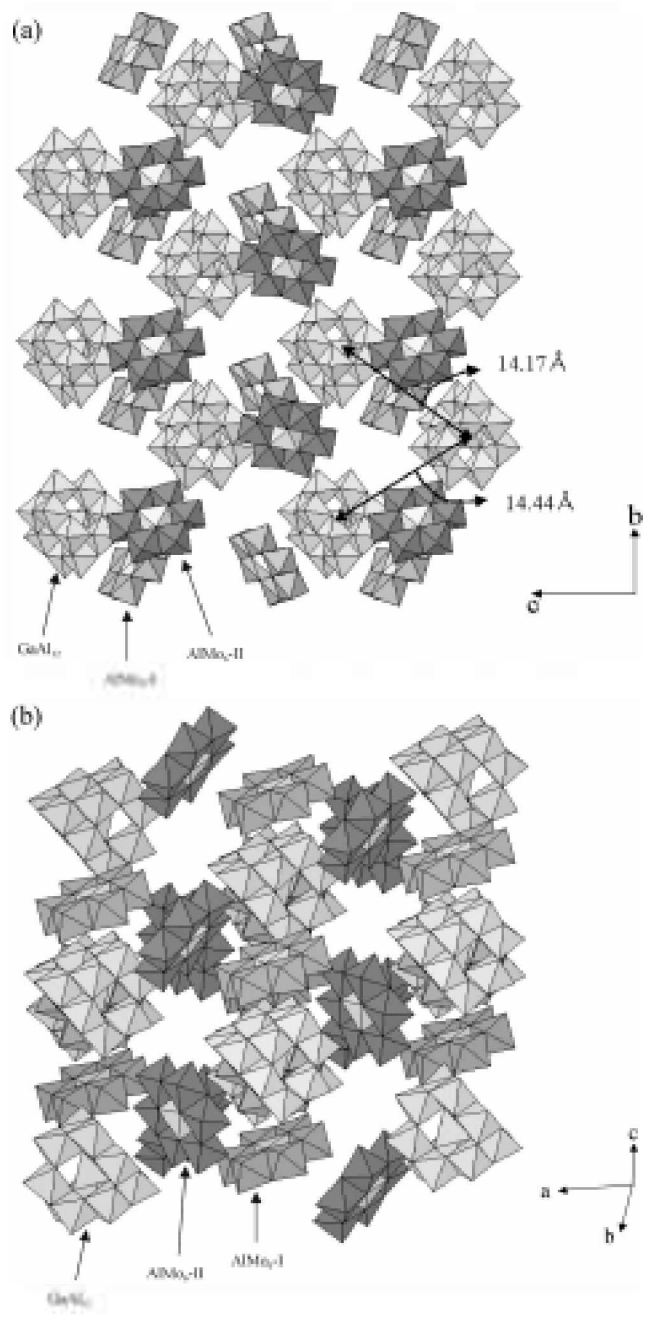

Figure 1. Crystal structure of $[GaO_4Al_{12}(OH)_{24}(H_2O)_{12}][Al(OH)_6Mo_6O_{18}]_2(OH)\cdot 30H_2O$: (a) viewed perpendicularly to the *bc*-plane and (b) along the [011] direction of the monoclinic unit cell showing channels. $GaAl_{12}$, $AlMo_6$-I and $AlMo_6$-II clusters are shown as white, gray and dark polyhedra, respectively.

(shown in Figure 1) is composed of $GaAl_{12}$ and $AlMo_6$ clusters in 1 : 2 ratio. There are two crystallographically different $AlMo_6$ clusters. and these will be denoted as $AlMo_6$-I and $AlMo_6$-II. The crystal structure can be described with alternating layers of $GaAl_{12}$-$AlMo_6$-I and $AlMo_6$-II stacked along the *a*-axis. The $AlMo_6$-II clusters can be considered as pillars between adjacent $GaAl_{12}$-$AlMo_6$-I layers leaving two dimensional crosslinked channels running parallel to the *bc*-plane. The lattice water and OH^- are located in these channels. There are four such layers in the unit cell along the *a*-axis and only two alternating layers are shown in this figure. The $GaAl_{12}$-$AlMo_6$-I layer can be described with zigzag chains formed by $GaAl_{12}$ and $AlMo_6$-I clusters alternating along the direction of *c*-axis. The structure of $GaAl_{12}$ cluster can be approximated as a truncated tetrahedron with six H_2O and six OH groups bonded to Al atoms forming a plane at each of the four wide faces of the truncated tetrahedron. Figure 2. On the other hand. the structure of $AlMo_6$ clusters can be regarded as a plate with three OH groups and nine O atoms forming a plane on each side of the cluster. Figure 3. The zigzag chain can be understood as packing of the $GaAl_{12}$ and $AlMo_6$-I clusters with their flat faces almost parallel to each other. These chains are packed along the *b*-direction to form a layer parallel to the *bc*-plain of the unit cell. The oxygen plains of contacting $GaAl_{12}$ and $AlMo_6$-I clusters are almost parallel to each other with a tilting angle of 2.4(1)°. The crystal structure of **1** gave this value 2.7(1)°.[5] This is understandable considering the ionic nature of inter-cluster interactions. In order to optimize the ionic interactions, the $GaAl_{12}$ and $AlMo_6$-I clusters have to get as close as possible to each other. But not all the twelve oxygen atoms of a cluster's face are in close contact with those of the other cluster ion's face. The crystal structure shows eight pairs of oxygen atoms, one from $GaAl_{12}$ and the other from $AlMo_6$-I with O-O separation shorter than 3.0 Å, suggesting that hydrogen bondings of these oxygen pairs are important interactions in addition to the aforementioned ionic interactions (Figure 4).

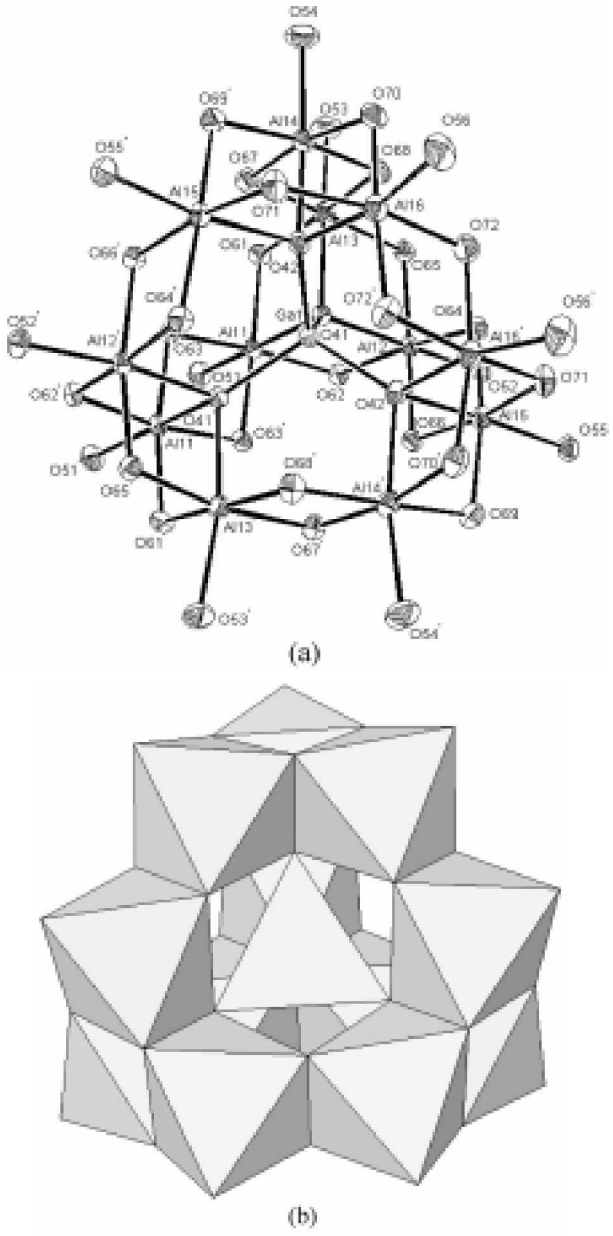

Figure 2. ORTEP and polyhedral drawings of the $[GaO_4Al_{12}(OH)_{24}(H_2O)_{12}]^{7-}$ cluster ion in the crystal structure of $[GaO_4Al_{12}(OH)_{24}(H_2O)_{12}][Al(OH)_6Mo_6O_{18}]_2(OH)\cdot 30H_2O$.

Between the packed chains are narrow zigzag channels with channel dimensions of 1.6 Å for the narrowest and 3.6 Å for the widest.[13] The distance between Ga centers is 14.17 Å between the two adjacent $GaAl_{12}$ clusters within the same chain and 14.44 Å between the Ga centers of adjacent chains. For comparison. the corresponding distances between tetrahedral Al centers of Al_{13} in **1** are 14.47 Å and 14.57 Å, respectively.

$GaAl_{12}$ adopts the *ε*-isomer structure among the five possible isomers of the Keggin-type structures, with its four edge sharing M_3O_{13} triads again sharing edges to each other.[14] The details of the $GaAl_{12}$ cluster structure of crystal **2** show slight variations from the literature data probably because of the lower symmetry of our crystal than the literature one of *F*-43*m* (Table 3).[9] The terminal oxygens (O51-O56) for H_2O groups have Al-O bond lengths 1.898(3)-1.947(4) Å. slightly shorter than the literature value of 1.962(6) Å. The double bridge oxygens (O61-O72) for OH groups with Al-O bond length 1.837(4)-1.930(3) Å show wider distribution than those in the literature, 1.852(6) and 1.869(7) Å. The four quarternary bridging oxygens in the central tetrahedron (O41 and O42) have Al-O bond length 1.981(3)-2.021(4) Å and are close to those in the literature. 2.009(6) Å. The larger Ga atom in the central T_d position gives rise to longer Ga-O bonds (1.878(3), 1.889(3) Å) than the corresponding Al-O bonds (1.859(7), 1.880(7) Å) of Al_{13} in **1**. The peripheral Al atoms in both clusters have almost identical local geometries, with the $GaAl_{12}$ having slightly more distorted O-Al-O angles (77.8(2)-171.94(16)°) and shorter Al-O bond length (1.837(4)-2.021(4) Å) than Al_{13} (78.8(3)-173.4(3)° and 1.873(7)-2.115 (7) Å) in **1** because of the large Ga atom than Al in the center.

$AlMo_6$ is a member of the Anderson-type heteropolyoxo-

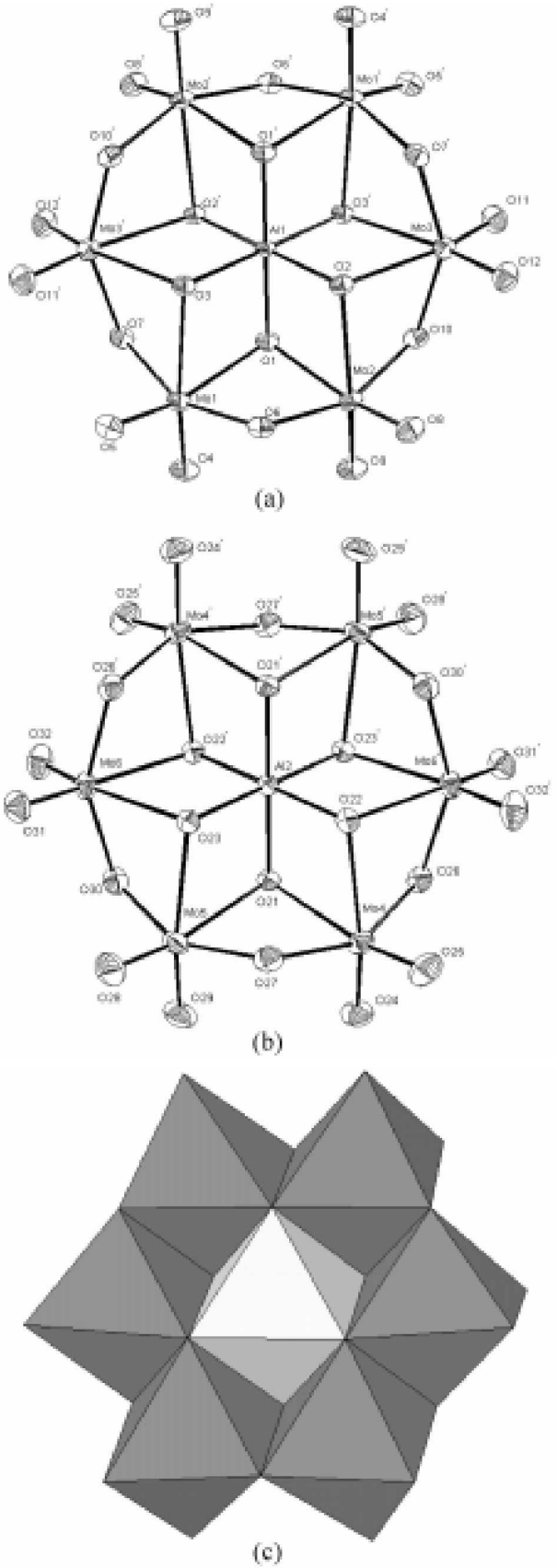

Figure 3. ORTEP and polyhedral drawings of the $[Al(OH)_6Mo_6O_{18}]^{3-}$ cluster ion in the crystal structure of $[GaO_4Al_{12}(OH)_{24}(H_2O)_{12}][Al(OH)_6Mo_6O_{18}]_2(OH)\cdot 30H_2O$. (a) $AlMo_6$-I and (b) $AlMo_6$-II.

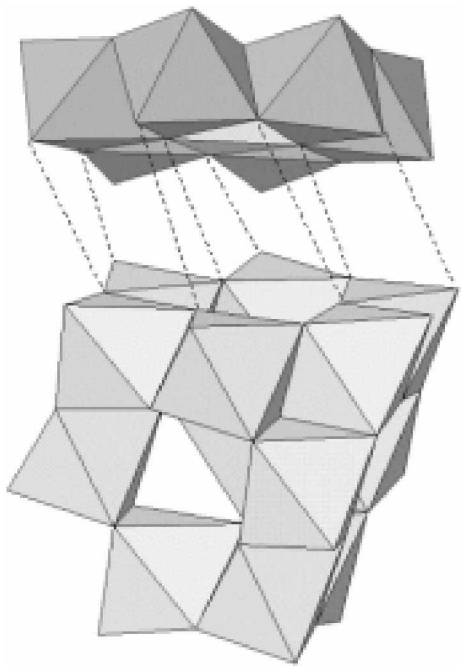

Figure 4. Hydrogen bonding scheme between oxygen atoms of adjacent $GaAl_{12}$ and $AlMo_6$-I clusters. Hydrogen bondings between the oxygen atoms are shown by dashed lines: O12-O69, O7-O55, O8-O67, O2-O66, O1-O52, O6-O63, O3-O62, O5-O51, from left to right.

metalates in which many different elements such as Fe, Co and Cr can be substituted in the central octahedral position.[15] The two $AlMo_6$ clusters in **2** show slight variations with $AlMo_6$-I having more distorted structure from the reported.[16] The Al-OH bonds in the central $Al(OH)_6$ octahedron are in the range of 1.898(3)-1.920(3) Å for $AlMo_6$-I (Al1 to O1-O3) and 1.895(3)-1.902(3) Å for $AlMo_6$-II (Al2 to O21-O23). Similarly, the terminal Mo=O bond lengths are 1.701(4)-1.732(4) Å for $AlMo_6$-I and 1.701(5)-1.712(4) Å for $AlMo_6$-II. More importantly, the Mo-OH bonds of $AlMo_6$-I have wider spread with 2.128(3)-2.321(3) Å than those of $AlMo_6$-II with 2.271(3)-2.310(3) Å. The distinctively short Mo-OH bonds around O1 atom (2.153(3) and 2.128(3) Å) than the others of about 2.3 Å may raise a question whether this oxygen is indeed a OH ligand. Bond valence sum (BVS) calculation on the oxygen atoms of these clusters shows that O1 has BVS = 1.58 while the other oxygens for OH ligands have BVS = 1.18-1.23.[17] The difference from the ideal value of 2.0 can be attributed to the bonds to H atoms. The larger BVS for O1 than the other equivalent oxygen atoms of OH ligands may be taken as an evidence for stronger hydrogen bonding for O1. That is, by forming a strong hydrogen bonding, the O1-H bond is weakened rendering O1 a higher bond valence to form stronger bonds with surrounding metal atoms. Indeed, this oxygen has a very short O-O distance of 2.604(5) Å with O52 for a H_2O ligand in the adjacent $GaAl_{12}$ while the other O-O distances for intercluster hydrogen bondings are in the range of 2.657(5)-3.002(5) Å. (Table 4) An alternative explanation for the short O1-Mo bonds would be that O1 is deprotonated. Unfortunately, the diffraction

Table 3. Selected bond lengths [Å] for $[GaO_4Al_{12}(OH)_{24}(H_2O)_{12}][Al(OH)_6Mo_6O_{18}]_2(OH)\cdot 30H_2O$

Mo(1)-O(4)	1.707(4)	Al(1)-O(3)	1.920(3)
Mo(1)-O(5)	1.732(4)	Al(1)-O(3)#1	1.920(3)
Mo(1)-O(6)	1.940(4)	Al(2)-O(21)#4	1.895(3)
Mo(1)-O(7)	1.952(4)	Al(2)-O(21)#3	1.895(3)
Mo(1)-O(1)	2.153(3)	Al(2)-O(23)#4	1.896(3)
Mo(1)-O(3)	2.321(3)	Al(2)-O(23)#3	1.896(3)
Mo(2)-O(9)	1.706(4)	Al(2)-O(22)#4	1.902(3)
Mo(2)-O(8)	1.724(4)	Al(2)-O(22)#3	1.902(3)
Mo(2)-O(10)	1.938(4)	Al(11)-O(61)	1.850(3)
Mo(2)-O(6)	1.963(4)	Al(11)-O(63)#3	1.853(3)
Mo(2)-O(1)	2.128(3)	Al(11)-O(63)	1.864(3)
Mo(2)-O(2)	2.314(3)	Al(11)-O(62)	1.887(3)
Mo(3)-O(11)	1.701(4)	Al(11)-O(51)	1.944(4)
Mo(3)-O(12)	1.710(4)	Al(11)-O(41)	2.000(3)
Mo(3)-O(10)	1.922(4)	Al(12)-O(65)	1.847(3)
Mo(3)-O(7)#1	1.930(3)	Al(12)-O(64)	1.847(3)
Mo(3)-O(3)#1	2.276(3)	Al(12)-O(62)	1.896(3)
Mo(3)-O(2)	2.285(3)	Al(12)-O(52)	1.898(3)
Mo(4)-O(25)	1.704(4)	Al(12)-O(66)	1.909(3)
Mo(4)-O(24)	1.710(4)	Al(12)-O(41)	1.997(3)
Mo(4)-O(27)	1.928(4)	Al(13)-O(68)	1.856(4)
Mo(4)-O(26)	1.930(4)	Al(13)-O(65)	1.860(3)
Mo(4)-O(21)	2.284(3)	Al(13)-O(67)	1.866(4)
Mo(4)-O(22)	2.301(3)	Al(13)-O(61)	1.875(4)
Mo(5)-O(29)	1.702(4)	Al(13)-O(53)	1.918(4)
Mo(5)-O(28)	1.710(4)	Al(13)-O(41)	1.998(3)
Mo(5)-O(27)	1.922(4)	Al(14)-O(68)	1.849(4)
Mo(5)-O(30)	1.942(4)	Al(14)-O(70)	1.862(4)
Mo(5)-O(23)	2.271(3)	Al(14)-O(67)	1.868(4)
Mo(5)-O(21)	2.310(3)	Al(14)-O(69)#3	1.873(4)
Mo(6)-O(32)	1.701(5)	Al(14)-O(54)	1.932(4)
Mo(6)-O(31)	1.712(4)	Al(14)-O(42)	1.993(4)
Mo(6)-O(30)	1.919(4)	Al(15)-O(64)	1.837(4)
Mo(6)-O(26)#2	1.945(4)	Al(15)-O(69)	1.849(4)
Mo(6)-O(22)#2	2.286(3)	Al(15)-O(71)	1.857(4)
Mo(6)-O(23)	2.310(3)	Al(15)-O(66)	1.930(3)
Ga(1)-O(42)#3	1.878(3)	Al(15)-O(55)	1.947(4)
Ga(1)-O(42)	1.878(3)	Al(15)-O(42)#3	1.981(3)
Ga(1)-O(41)	1.889(3)	Al(16)-O(72)#3	1.839(4)
Ga(1)-O(41)#3	1.889(3)	Al(16)-O(70)	1.849(4)
Al(1)-O(1)#1	1.898(3)	Al(16)-O(72)	1.868(4)
Al(1)-O(1)	1.898(3)	Al(16)-O(71)#3	1.873(4)
Al(1)-O(2)	1.910(3)	Al(16)-O(56)	1.935(4)
Al(1)-O(2)#1	1.910(3)	Al(16)-O(42)	2.021(4)

Symmetry transformations used to generate equivalent atoms: #1 -x,-y+1,-z−1 #2 -x-1/2,-y−1/2,-z+1 #3 -x,y,-z−1/2 #4 x−1/2,-y+1/2,z-1/2

data alone cannot provide any strong evidence for either model. However, we think the second possibility is not likely because such deprotonation will make the charge of the cluster −5 instead of −3. Such a drastic change of charge would be reflected in many aspects of the cluster structure. which is not the case. Moreover, the crystal structure **1** show the same feature of short O1-Mo bonds of $AlMo_6$-I cluster. whose −3 charge is well established by the charge balance

Table 4. Distances between hydrogen bonded oxygen atoms [Å] for $[GaO_4Al_{12}(OH)_{24}(H_2O)_{12}][Al(OH)_6Mo_6O_{18}]_2(OH)\cdot 30H_2O$

Between $AlMo_6$-I and $GaAl_{12}$		Between $AlMo_6$-II and $GaAl_{12}$	
O1-O52	2.604(5)	O24-O55	2.807(5)
O2-O66	2.736(4)	O26-O52	2.703(5)
O3-O62	2.744(5)		
O5-O51	2.801(5)	Between $AlMo_6$-I and $AlMo_6$-II	
O6-O63	3.002(5)	O4-O21	2.704(5)
O7-O55	2.657(5)	O9-O23	2.673(5)
O8-O67	2.745(5)		
O12-O69	2.766(5)		

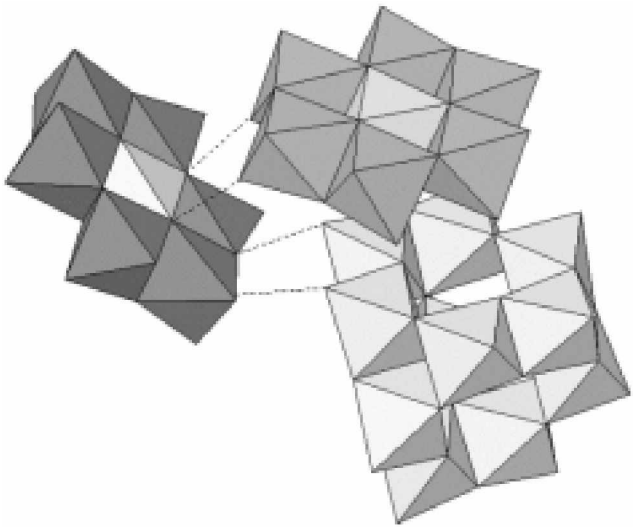

Figure 5. Hydrogen bondings between oxygen atoms of a $AlMo_6$-II clusters with oxygen atoms of neighboring clusters. Hydrogen bondings between the oxygen atoms are shown by dashed lines : O9-O23, O4-O21, O26-O52, O24-O55, from top to bottom.

consideration including a OH^- ion inside the channel. (below) Therefore, we conclude that the unusually short O1-Mo distances are induced by the strong hydrogen bond involving O1 atom according to the first model.

Though the structure was explained with separate layers of $GaAl_{12}$-$AlMo_6$-I and $AlMo_6$-II. the layers are closely related to each other by hydrogen bondings also as discussed just above. The $AlMo_6$-II pillars are not oriented perpendicularly (with their wide oxygen planes perpendicularly) to the *bc*-plane, but much tilted with respect to the *bc*-plane to link the $GaAl_{12}$ and $AlMo_6$-I clusters of the two adjacent $GaAl_{12}$-$AlMo_6$-I planes by hydrogen bondings. Four oxygen atoms in one face of $AlMo_6$-II are in hydrogen-bonding distance with adjacent $GaAl_{12}$ and $AlMo_6$-I clusters (Figure 5). A terminal and a μ_2-OH oxygen atoms of $AlMo_6$-II are in hydrogen-bonding distance to the $GaAl_{12}$ cluster. and two oxygen atoms of central octahedron of $AlMo_6$-II are in hydrogen bonding distance to terminal oxygen atoms of $AlMo_6$-I. It is interesting to note that $AlMo_6$-I and $AlMo_6$-II are directly hydrogen bonded, even though they have the same sign of charge. indicating that the ionic term is not strictly applied in the packing of the cluster ions. The hydrogen bondings in these crystals **1** and **2** are between two

OH groups or between a OH and a H_2O group, which appears to be not feasible because of steric hindrance with more than one intervening hydrogen atoms between the two hydrogen bonded oxygen atoms. However, a close inspection of the local environments of the oxygen atoms involved in the hydrogen bondings suggest that one of the two oxygen atoms involved in a hydrogen bonding (mostly those in the $GaAl_{12}$ cluster) is oriented in such a way to direct its sp^3 lone pair toward the other oxygen atom to enable a hydrogen bonding between them.

The two types of clusters, $GaAl_{12}^{7-}$ and $AlMo_6^{3-}$ in 1 : 2 ratio, identified from the structure determination do not balance their charges. This imbalance may be resolved if one of the H_2O ligands of the $GaAl_{12}$ cluster is, in fact, deprotonated and the cluster has a charge 6+ instead of 7+. Although the $GaAl_{12}$ clusters are not well studied for this aspect, its analogue Al_{13} clusters, reportedly, can have lower charges than 7+ at higher pH's.[18] Alternatively, incorporation of OH^- ions inside the channel to make the composition $(GaAl_{12})(AlMo_6)_2(OH)$ can resolve the charge imbalance problem as in the crystal **1**. In the latter, the OH^- ion was unambiguously identified from the 188 K crystal data because the oxygen atom of the OH^- ion showed different environment from those of the water molecules inside the channel. Although almost the same number of oxygen atoms were found and refined inside the channel, the crystal structure of **2** did not reveal any unique oxygen position for OH^-, probably because of the larger thermal motions of channel water molecules and OH^- ions at room temperature at which the present diffraction data were collected. Nevertheless, we believe that the OH^- ions are present in crystal **2** based on following considerations: First, the two crystal structures are almost identical. The deprotonation suggested in the first possibility would cause detectable structural changes of the $GaAl_{12}$ cluster from the Al_{13}, which is not the case. Second, the almost same amounts of oxygen atoms inside the channels of crystal **1** and crystal **2** indicate that the channels of the crystals have almost the same sizes, an evidence that the two crystals are chemically identical except for the replacement of $GaAl_{12}$ for Al_{13}. Accordingly, we report the chemical formula of crystal **2** with a OH^- ion as shown in the title.

We have observed degradation of crystal over a period of three to four days during data collection of **1**. Therefore the crystal data for crystal **1** were collected on a CCD diffractometer at 188 K. On the contrary, the crystal **2** exhibited considerably higher stability, which enabled us to collect the crystal data on a four-circle diffractometer at room temperature. The better stability of compound **2** over compound **1** may be related with the better stability of $GaAl_{12}$ over Al_{13} as mentioned before. Different stability of $GaAl_{12}$ over Al_{13} is expected to give rise to different microstructures of corresponding nanocomposites to be formed.

Conclusion

In this paper, we report the synthesis and crystal structure of a new nanocomposite $[GaO_4Al_{12}(OH)_{24}(H_2O)_{12}][Al(OH)_6$-$Mo_6O_{18}]_2(OH)\cdot 30H_2O$, an analogue of $[AlO_4Al_{12}(OH)_{24}$-$(H_2O)_{12}][Al(OH)_6$-$Mo_6O_{18}]_2(OH)\cdot 29.5H_2O$. The disposition of the cluster ions appear to be governed by the three important inter-cluster interactions: ionic interactions to put oppositely charged clusters as close as possible, hydrogen bondings between the OH^-, O^{2-} and H_2O ligands of the clusters surface, and probably the optimal packing principle. The two isostructural compounds **1** and **2** are the first example that shows interplay of these three interactions in one crystal structure.

Acknowledgment. This research was supported from KOSEF through the CNNC SRC at SKKU.

References

1. (a) Wen, J.; Wilkes, G. L. *Chem. Mater.* **1996**, *8*, 1667. (b) Hulteen, J. C.; Martin, C. R. *J. Mater. Chem.* **1997**, *7*, 1075. (c) Choy, J.-H.; Kwak, S.-Y.; Park, J.-S.; Jeong, Y.-J.; Portier, J. *J. Am. Chem. Soc.* **1999**, *121*, 1399. (d) Forster, S.; Antonietti, M. *Adv. Mater.* **1998**, *10*, 195.
2. (a) Buttry, D. A. *Langmuir* **1999**, *15*, 669. (b) Gomez-Romero, P. *Adv. Mater.* **2001**, *13*, 163. (c) Molina, C.; Dahmouche, K.; Ribeiro, S. J. L. *J. Phys. Chem. B* **2001**, *105*, 3378. (d) Weller, H. *Angew. Chem. Int. Ed.* **1998**, *37*, 1658. (e) Petit, L.; Sellier, E.; Duguet, E. *J. Mater. Chem.* **2000**, *10*, 253. (e) Lvov, Y.; Ariga, K.; Ichinose, I.; Kunitake, T. *Langmuir* **1996**, *12*, 3038.
3. (a) Sanz, N.; Ibanez, A. *Appl. Phys. Lett.* **2001**, *78*, 2571. (b) Mulvaney, P.; Liz-Marzán, L. M.; Giersig, M. *J. Mater. Chem.* **2000**, *10*, 1259.
4. Choi, H.; Kwon, Y.-U.; Han, O. H. *Chem. Mater.* **1999**, *11*, 1641.
5. Son, J. H.; Choi, H.; Kwon, Y.-U. *J. Am. Chem. Soc.* **2000**, *122*, 7432.
6. (a) Ohman, L.-O. *Inorg. Chem.* **1989**, *28*, 3629. (b) Carrier, X.; Lambert, J. F.; Che, M. *J. Am. Chem. Soc.* **1997**, *119*, 10137.
7. Son, J. H.; Choi, H.; Kwon, Y.-U.; Han, O. H. to be published.
8. (a) Allouche, L.; Gerardin, C.; Loiseau, T.; Ferey, G.; Taurelle, F. *Angew. Chem. Int. Ed.* **2000**, *39*, 511. (b) Rowsell, J.; Nazar, L. F. *J. Am. Chem. Soc.* **2000**, *122*, 3777.
9. Parker, W. O.; Millini, R.; Kiricsi, I. *Inorg. Chem.* **1997**, *36*, 571.
10. Johansson, G. *Acta Chem. Scand.* **1960**, *14*, 771.
11. Sheldrick, G. M. SHELXS-86; University of Gottingen: 1986.
12. Sheldrick, G. M. SHELXL-97-2: University of Gottingen: 1997.
13. These values were calculated from the distances between nearest oxygen atoms minus the van der Waals radii of oxygen atoms (1.40 Å).
14. (a) Baker, L. C. W.; Figgis, J. S. *J. Am. Chem. Soc.* **1970**, *92*, 3794. (b) Keggin, J. F. *Nature* **1933**, *131*, 908.
15. (a) Baker, L. C. W.; Foster, G.; Tan, W.; Scholnick, F.; McCutcheon, T. P. *J. Am. Chem. Soc.* **1955**, *77*, 2136. (b) Perloff, A. *Inorg. Chem.* **1970**, *9*, 2228.
16. Lee, H. Y.; Park, K. M.; Lee, U.; Ichida, H. *Acta Cryst. C* **1991**, *47*, 1959.
17. Brown, I. D.; Altermatt, D. *Acta Cryst. B* **1985**, *41*, 244.
18. Furrer, G.; Ludwig, C.; Schindler, P. W. *J. Colloid Interface Sci.* **1992**, *149*, 56.